Unidirectional recruitment is essential for viral latency

Ido Lavi[#], Supriya Bhattacharya[#], Ola Orgil, Ankita Awase, Nir Avital, Guy Journo, Vyacheslav Gurevich and Meir Shamay*

Daniella Lee Casper Laboratory in Viral Oncology, Azrieli Faculty of Medicine, Bar-Ilan University, Safed, Israel 1311502

[#] These authors contributed equally to this work

* Corresponding author

Meir Shamay

Email: meir.shamay@biu.ac.il

Running Title: Unidirectional recruitment of LANA by MeCP2

Author Contributions: Conceived and designed the experiments: I.L., S.B., M.S. Performed the experiments: I.L., S.B., A.A, Analyzed the data: I.L., S.B., G.J. & M.S. Generated tools & reagents: O.O., N.A., V.G., S.B., Wrote the paper: M.S.

Preprint Servers:

Classification: Biological sciences, Microbiology.

Competing Interest Statement: The authors declare no competing financial interests.

Keywords: CRISPR/Cas9, dCas9, KSHV, HHV-8, LANA, MeCP2, Recruitment.

Abstract

Kaposi's sarcoma associated herpesvirus (KSHV, HHV-8) is associated with several human malignancies. During latency the viral genomes reside in the nucleus of infected cells as large non-integrated plasmids, known as viral episomes. All KSHV infected cells express LANA, and LANA is essential for viral latency. LANA binding to the viral episomes is critical both for replication of the viral genomes during latency, and for tethering the viral episomes to the cell chromosomes during cell division. Directional recruitment of protein complexes are critical for proper function of many nuclear processes. To test for recruitment directionality between LANA and cellular proteins we directed LANA via catalytically inactive Cas9 (dCas9) to a repeat sequence to obtain easily detectable dots. Then, recruitment of nuclear proteins to these dots can be evaluated. We found that LANA recruited its known interactors ORC2 and SIN3A. Interestingly, LANA was unable to recruit MeCP2, but MeCP2 recruited LANA. Similarly, histone deacetylase 1 (HDAC1) that interact with the transcriptional-repression domain (TRD) of MeCP2, same as LANA, was unable to recruit MeCP2, but MeCP2 was able to recruit HDAC1. In contrast, HP1α that interacts with MeCP2 through a different domain, was able to recruit MeCP2. We propose that available interacting domains in DNA bound/dimerized form of MeCP2, forces this recruitment directionality. We found that cells derived from Rett syndrome and express a mutant MeCP2 (T158M), impaired in DNA binding, cannot support KSHV genome maintenance. Therefore, this unidirectional recruitment of LANA by MeCP2 identified MeCP2 as a critical factor for viral maintenance.

Significance Statement

Using a CRISPR/Cas9 recruitment assay, we show that some interacting proteins have a unidirectional recruitment property, where only one of the proteins can recruit its partner. We found unidirectional recruitment relations between the methylated DNA binding protein MeCP2 and KSHV encoded LANA. Where MeCP2 recruits LANA, but LANA is unable to recruit MeCP2. Similarly, MeCP2 recruits histone deacetylase 1 (HDAC1), but HDAC1 is unable to recruit MeCP2. We propose that this unidirectional recruitment is the result of available interacting domains. Furthermore, this unidirectional recruitment seems to be critical for viral latency, since LANA fails to maintain the viral genomes in MeCP2 mutant cells. Therefore, in this case unidirectional recruitment is a matter of survival or extinction.

Introduction

Kaposi's sarcoma associated herpesvirus (KSHV, HHV-8) is the causative agent of all forms of Kaposi's sarcoma (KS), and is tightly associated with primary effusion lymphoma (PEL), and multicentric

Castleman's disease (1, 2). Like all herpes viruses KSHV has two phases: latent (dormant) and lytic (productive) cycle. During latency the viral genomes reside in the nucleus of infected cells as large non-integrated plasmids, known as viral episomes. All KSHV infected cells express LANA, and LANA is essential for viral latency (3-5). LANA binding to the viral episomes is critical both for replication by recruitment of the cellular replication machinery to the viral genomes (6, 7), and for maintenance by tethering the viral episomes to the cell chromosomes during cell division (8, 9). Both the N and C-terminal regions of LANA have been shown to mediate chromosome association; the N-terminal via binding to core histones H2A and H2B (10), while for the C-terminal several candidates were identified including MeCP2, DEK and RING3 (11-13). Multiple LANA binding sites (LBS1 and LBS2) (14, 15) within the KSHV terminal repeats, and its oligomerization ability (16, 17) create clearly visible LANA dots in KSHV-infected cells. In contrast, LANA is equally distributed in the nucleus when it is expressed in un-infected cells. So, it is challenging to determine whether LANA or the viral genomes are the recruiters of cellular factors.

For many nuclear processes directional recruitment of protein complexes is critical for proper function. Transcription factor that binds a specific DNA sequence recruits co-activators and general transcription factors that results in subsequent recruitment of RNA polymerase leading to gene expression. In this scenario, it is expected that a transcription factor of interest will recruit the co-activator. However, the co-activator that is recruited by other transcription factors as well, should not recruit the transcription factor of interest. One example of recruitment directionality is the estrogen receptor, where the combination of ligand binding, dimerization and sequence specific DNA binding are required to generate high affinity surface to recruit co-activator proteins (18). This conformational change upon DNA binding and dimerization will favor binding and recruitment of co-activator to enhancer/promoter bound receptor and minimize interaction with DNA-free receptor.

MeCP2 binds methylated DNA and recruits co-repressor complexes to execute the readout of CpG methylation into transcription repression (19). Several studies detected interaction between MeCP2 and histone deacetylase 1 (HDAC1), and recruitment of histone deacetylase activity plays a role in transcription repression imposed by MeCP2 (20, 21). MeCP2 and HDAC1 represent an example of two proteins that interact in the nucleus. While MeCP2 recruits HDAC1 to methylated regions in order to repress transcription, we expect that HDAC1 should not recruit MeCP2 to promoters in those cases where HDAC1 is recruited by other transcription factors. Another protein that plays important role in transcription repression is heterochromatin protein 1 (HP1). HP1 interacts with the repressive mark histone 3 lysine 9 tri-methylation (H3K9Me3) and via recruitment of SUV39H1, the histone H3K9Me3 methyltransferase,

leads to spreading of this heterochromatin repressive histone mark (22, 23). HP1 has been shown to interact with MeCP2 (24, 25), but whether HP1 can recruit MeCP2 is an open question.

Cas9 is an endonuclease that can be directed to different DNA targets that are complimentary to a guide RNA and contain a PAM sequence (26). Soon after the discovery of this property, many applications of this sequence specific targeting of Cas9 emerged. For targeting purposes, the endonuclease is no longer needed, and a catalytically dead mutant Cas9 (dCas9) that still retains DNA binding capability was created (26, 27). Targeting this dCas9 to promoter sequences results in transcription activation or repression depending on the fused domains and the targeting location relative to the transcription start site (27, 28). Shortly after the creation of the dCas9 it was directed to repeat elements for the visualization of these elements in fixed (29) and live cells (30-32).

Here we harness CRISPR/Cas9 to determine recruitment relations between LANA and cellular proteins. We termed this method CRISPR-PITA, for Protein Interaction and Telomere recruitment Assay. We combined the ability of the SunTag system (33) to gather up to ten molecules of a protein of interest with CRISPR/dCas9 targeted to a repeat sequence such as telomeres. The ability of this protein to recruit endogenous or fluorescently tagged proteins to these telomere dots is determined. Interestingly, we find that the recruitment does not always work bi-directionally. LANA fails to recruit MeCP2, but MeCP2 efficiently recruits LANA. The unidirectional recruitment of LANA by MeCP2 raised the possibility that MeCP2 may serve as a protein anchor for LANA tethering. Indeed, we found that the virus fails to maintain its episomes in cells expressing a mutant MeCP2. We hypothesized that the interaction domain will only become available for interaction with LANA upon binding to DNA. To test this, we performed recruitment assay of MeCP2 by LANA in the presence of a short DNA oligo with MeCP2 binding site. Interestingly, now LANA was able to recruit MeCP2. We propose that available interacting domains can determine recruitment directionality.

Results

Creation of visible dots at the telomeres with dCas9-SunTag and scFv-LANA

The KSHV encoded LANA localizes in large dots together with the viral episomes in KSHV infected cells but is equally distributed in the nucleus when expressed in un-infected cells (34). In order to test recruitment directionality between LANA and nuclear proteins we were interested to create LANA dots in un-infected cells. The ability of dCas9 to direct proteins of interest to any genomic locus makes it an ideal system for a recruitment assay. In order to enhance dot formation, we utilized the SunTag system where tandem epitopes

can concentrate multiple molecules of an antibody-fused protein that recognizes this epitope (up-to 10 with the tag used in this study) (33). In our case the tandem epitopes are fused to dCas9 and the antibody scFv is fused to our protein of interest (**Fig. 1A**). Transfection of LANA fused with the antibody scFv (scFv-LANA) together with dCas9 and sgRNA for telomere repeat sequence, resulted in LANA-telomere-dots that were visible by immuno-fluorescent assay (IFA) for LANA (**Fig. 1B**). When the dCas9 was omitted from the mix LANA could not generate nuclear dots, suggesting that LANA-telomere-dots are dependent on the targeting of LANA to telomeres via dCas9. To validate that LANA was targeted to the telomeres we used an antibody against the telomeric repeat factor 2 (TRF2), and indeed scFv-LANA co-localized with TRF2 when co-transfected with dCas9 and sgTelomere (**Fig. S1**). The larger dots of TRF2 observed where it colocalize with LANA, can be explained by LANA's ability to oligomerize (14, 16, 17, 35, 36). Studies of the LANA oligomerization property identified a LANA oligomerization mutant (16, 17). Therefore, we created this LANA oligomerization mutant (F1037A/F1041A) in the context of scFv-LANA (scFv-LANA-mutant) and compared the dot size to scFv-LANA. As expected, the LANA oligomerization mutant created smaller telomere dots compared to wt LANA of both LANA and TRF2 (**Fig. S1**). Altogether, these experiments indicate that we can generate LANA dots in un-infected cells using the dCas9 SunTag system.

LANA recruits ORC2 and SIN3A but not MeCP2

In this assay a protein of interest is targeted to telomeres via dCas9, and the recruitment of endogenous proteins to these dots is detected by immunofluorescence assay (**Fig. 1C**). We termed this method CRISPR-PITA for Protein Interaction and Telomere recruitment Assay. We performed the CRISPR-PITA assay for ORC2, a subunit of the Origin Replication Complex (ORC), previously reported to interact with LANA and localize with LANA-episome-dots (17, 37-39). ORC2 was recruited by LANA, as was determined by the easily detected dots that co-localized with LANA (**Fig. 2A**), and the overlapping fluorescence intensity peaks along the arrow line (on the right side of the images). It is important to note, that while the dCas9 and scFv-LANA were ectopically expressed, the recruited proteins are endogenous proteins, indicating the ability of LANA to recruit the endogenous ORC2.

Several studies reported on interaction between LANA and the corepressor protein SIN3A (mSin3a) (39, 40), and the methyl-CpG binding protein MeCP2 (11, 12, 41), but it was reported that MeCP2 is not associated with LANA dots in KSHV infected cells (42). We found that scFv-LANA recruited SIN3A to LANA-telomere-dots, both by the visual observation of the dots and the fluorescence intensity plot (**Fig. 2B**). Analysis of MeCP2 recruitment via the CRISPR-PITA revealed no recruitment of MeCP2 to LANA-telomere-dots (**Fig. 2C**). We also determined the Pearson's correlation coefficient for the different

147 treatments (**Fig. 2D**). When LANA alone is transfected, there should be an overlap between LANA and
148 these proteins, as they are known LANA interactors. When LANA is targeted to the telomeres via dCas9,
149 if LANA is able to recruit its partner, then the overlap is expected to remain or even increase. In contrast,
150 if LANA is unable to recruit its partner, the overlap should be reduced. This is exactly what we found when
151 we measured the Pearson's correlation coefficient for 15 cells in each experiment. The overlap was reduced
152 for the non-recruited MeCP2, remained the same for SIN3A, and increased for ORC2.

153 One possibility to explain the lack of MeCP2 recruitment by LANA, is that as a methylated DNA binding
154 protein, it is engaged in binding methylated DNA and therefore not available to be recruited by LANA. To
155 test this, we performed the CRISPR-PITA in cells with knock-out (KO) of DNMT1 and DNMT3b (HCT
156 DKO) that were reported to lose over 95% of their CpG methylation (43). Even in HCT DKO, scFv-LANA
157 could not recruit MeCP2 to LANA-telomere-dots (**Fig. S2**), suggesting that protein availability could not
158 explain the lack of recruitment in this case. Immunofluorescence assays for ORC2, SIN3A and MeCP2 in
159 KSHV-infected PEL (BCBL1) cells, revealed that while ORC2 and SIN3A were found associated with
160 LANA-episome-dots, MeCP2 was not associated with the LANA-episome-dots (**Fig. S3**), supporting the
161 ability of the CRISPR-PITA to predict recruitment ability between proteins.

162 **MeCP2 recruits LANA**

163 The observation that scFv-LANA could not recruit MeCP2, despite their documented interaction (11, 12,
164 41) highlights the importance to determine recruitment relations between proteins. Krithivas et al. have
165 shown that expression of human MeCP2 is able to recruit LANA to heterochromatin in NIH 3T3 mouse
166 cells (12). Therefore, we tested the ability of scFv-MeCP2 to recruit LANA to MeCP2-telomere-dots. Cells
167 were co-transfected with dCas9, sgTelomere, scFv-MeCP2 and expression vectors for GFP-LANA or GFP
168 alone as control. The scFv-MeCP2 was able to recruit GFP-LANA to MeCP2-telomere-dots, but not GFP
169 alone, supporting the ability of MeCP2 to recruit LANA (**Fig. 3A & B**). LANA contains three distinct
170 domains, the N-terminal region (AA 1-329), the C-terminal (AA 936-1162), and a middle repeat region.
171 Both the N and C-terminal regions have been shown to mediate chromosome association; the N-terminal
172 via binding to core histones H2A and H2B (10), while for the C-terminal several candidates were identified
173 including MeCP2, DEK and RING3 (11-13). To determine the region of LANA sufficient for recruitment
174 by MeCP2, we performed CRISPR-PITA by scFv-MeCP2 for LANA N+C, LANA N and LANA C. While
175 both LANA N+C and LANA C were efficiently recruited by MeCP2, no recruitment was observed with
176 the N-terminal (**Fig. 3C**). This result agrees with a previous study that located the interaction between
177 LANA and MeCP2 to the C-terminal region (11). Importantly, this result indicates that despite the high

concentration of the recruiter protein at telomeres, still CRISPR-PITA requires specific interaction, as both the N-terminal of LANA and GFP-alone were not recruited by MeCP2 in our assay.

Targeting dCas9 to a repeat element, results in high protein concentration at specific nuclear locations. One concern that might be raised is whether the recruitment we observed with CRISPR-PITA is specific or an artifact of the high protein concentration. To rule out this possibility, we directed dCas9 to a single chromosomal location (at ERBB2 promoter) and followed the association of the proteins with this location by chromatin immunoprecipitation (ChIP) assay followed by qPCR (**Fig. 3D**). Here again we found that scFv-MeCP2 recruited more LANA to this promoter, while scFv-LANA failed to do the same for MeCP2. This result indicates that despite targeting dCas9 to a repeat sequence, the recruitment nicely reflects the recruitment by a single locus. This set of experiments highlights the distinction between interaction and recruitment, while LANA and MeCP2 were shown to interact with each other, still MeCP2 can recruit LANA, but LANA cannot recruit MeCP2.

MeCP2 recruits HDAC1, but HDAC1 is unable to recruit MeCP2

Several studies detected interaction between MeCP2 and histone deacetylase 1 (HDAC1), and this recruitment of histone deacetylase activity plays a role in transcription repression imposed by MeCP2 (20, 21). MeCP2 and HDAC1 represent an example where two proteins can interact to form protein complexes in the nucleus. We expect that MeCP2 should recruit HDAC1 to methylated regions in order to repress transcription, but HDAC1 should not recruit MeCP2 to the promoters where it is recruited by other transcription factors. Therefore, we applied the CRISPR-PITA to determine recruitment relations between these two cellular proteins. We found that scFv-MeCP2 efficiently recruits HDAC1 (**Fig. 4A**). In contrast, scFv-HDAC1 failed to recruit MeCP2 both in HCT (**Fig. 4B**) and HCT DKO cells (**Fig. 4C**). Thus, in the context of MeCP2 and HDAC1, recruitment is also unidirectional, enabling MeCP2 to recruit HDAC1 to repress transcription, but preventing the mislocalization of MeCP2 by HDAC1.

Availability of interacting domains determines recruitment directionality

A unidirectional recruitment between two interacting proteins is achieved when the interacting domain is available only upon certain conditions. In the case of MeCP2, it is expected that the transcriptional-repression domain (TRD) will be unavailable when it is a free protein in solution and becomes available for protein interaction only when MeCP2 is bound to DNA (**Fig. 5 C-D**). Both LANA and HDAC1 interact with the same region of MeCP2, the transcriptional-repression domain (TRD) and the methyl-CpG-binding domain (MBD) (35, 40). In contrast, Heterochromatin protein 1 (HP1α) interacts with the N-terminal

domain (amino acids 1–55) of MeCP2 (24) (**Fig. 5A**). We hypothesized that since HP1α interacts with a different domain that might be available for interaction also in its DNA-free state, HP1α might be able to recruit MeCP2. Interestingly, in CRISPR-PITA we found that scFv-HP1α was able to recruit MeCP2 (**Fig. 5B**).

This result supports the notion that available interacting domains determine recruitment directionality. To test this more directly, we performed recruitment assay of MeCP2 by scFv-LANA but now also provided a short double-strand (ds) DNA oligo with MeCP2 binding site. If our model is correct, MeCP2 will bind the oligo, make the interaction domain with LANA available, but now instead of binding cellular chromatin, it is bound to a short oligo and therefore can move around and be recruited by LANA. This is exactly what we observed when we transfected a short DNA oligo with MeCP2 binding site (**Fig. 5 E-F**). No recruitment was observed in un-transfected cells or cells transfected with a control DNA. This result supports the notion that LANA can interact only with a DNA bound MeCP2.

Rett syndrome mutant MeCP2 cannot support KSHV maintenance during latency

One important function of LANA is to maintain the viral episomal genomes, by tethering the viral genomes to cellular chromosomes during cell division, ensuring they remain in the nucleus once nuclear envelope is reformed. To do so, LANA directly binds the LANA binding sites (LBS1 and LBS2) (14, 15) on the viral genomes, and associates with cellular chromosomes. Our finding that MeCP2 recruits LANA, while LANA cannot recruit MeCP2 unless we provide a short oligo with MeCP2 binding site, suggests that the interaction with MeCP2 is permitted only once it is bound to methylated DNA, and therefore may be a potential candidate for LANA tethering. Sporadic mutations in MeCP2 are associated with most cases of Rett syndrome (RTT), a severe X-linked neurodevelopmental disorder in humans. (44). Lymphoblastoid Cell Lines (LCLs) derived from RTT patients expressing wild-type (wt) MeCP2 allele, mutant T158M (that cannot bind methylated DNA), and 803delG (deletion of the C' terminus) (**Fig. 5A**) of MeCP2 (45) were tested for their ability to support KSHV episome maintenance. Cells were infected with rKSHV (rKSHV.219) expressing GFP and maintenance of the viral episomal DNA and the percentages of GFP positive cells were analyzed (**Fig. 6 B & A**). While both wt and 803delG efficiently supported viral latency, the MeCP2 mutant in the MBD that cannot bind DNA (T158M) could not. This result indicates that a functional MeCP2 that is able to bind methylated DNA is essential for KSHV genome maintenance. LANA has been shown to bind both the MBD and TRD of MeCP2 (11). To determine if LANA can be recruited by the T158M mutant, we cloned it into scFv-MeCP2 and performed CRISPR-PITA assay. We found that MeCP2 T158M mutant can recruit LANA (although to a lesser extent), when it is artificially targeted to

chromatin by dCas9 (**Fig. 6C**). While the MBD deletion mutant, lost the ability to recruit LANA when artificially targeted to chromatin. To assay for both abilities, to recruit LANA and to bind methylated DNA, we harnessed a specific feature of MeCP2 to localize to heterochromatin loci in mouse cells. This assay is typically performed in NIH 3T3 cells, since they express very low levels of endogenous MeCP2 (12, 46). Similar to previous studies (11, 12), we found that LANA can be efficiently recruited to heterochromatin when co-transfected with wt MeCP2 (**Fig. 6D**). In contrast, both T158M and MBD-del mutants could not recruit LANA to heterochromatin loci. Altogether, we found that Rett syndrome mutant MeCP2 T158M, that cannot recruit LANA to methylated DNA, also cannot support KSHV episome maintenance. We revealed a critical role for MeCP2 in KSHV episome maintenance by LANA.

Discussion

A powerful method to study recruitment is the Chromatin immunoprecipitation (ChIP) assay, that can detect association of proteins with specific DNA sequences (47, 48). ChIP assays require fixation, proper shearing of the chromatin, and special antibodies that can perform the immunoprecipitation of the cross-linked chromatin. In many cases even when two or more proteins are associated with the same genomic region, it is hard to evaluate the relationship between the proteins and determine essential factors for the recruitment. Although this limitation can be overcome by using Knockout (KO) or Knockdown (KD) of one protein and testing the ability of other proteins to be recruited to DNA/chromatin in the absence of that protein, this raises additional challenges in creating KO or KD of the target gene. Another recruitment assay is based on integration of the *lac*O array into the genome and directing the protein of interest to this array via fusion to the Lac-repressor (49, 50). One limitation of this assay is the limited number of cell lines that were generated to contain integration of this *lac*O array.

Here we describe a simple method to test for recruitment relations between proteins. This method does not require chromatin shearing and can be performed with various antibodies that can recognize the native form of proteins, and in the absence of such an antibody a recruitment of fluorescently labeled proteins can be observed. To obtain visible dots we combined the ability of the repeated epitope SunTag with dCas9 targeted to a repetitive genomic sequence such as the telomeres. Although targeting dCas9 to telomeres has been performed previously to follow nuclear events such as, liquid–liquid phase separation (LLPS), or the generation of heterochromatin (51, 52), but has not been applied to test recruitment directionality. Using this method, we found unidirectional recruitment relations between proteins. Our results with CRISPR-PITA, indicated that LANA was able to recruit ORC2 and SIN3A, but was unable to recruit MeCP2 to LANA-telomere-dots. While it has been shown that ORC2 localizes with LANA dots (17, 37-39), and MeCP2 does not (42), there was no published data on SIN3A localization in KSHV infected cells. So, we

271 performed immunofluorescence assay in KSHV-infected BCBL1 cells and found that both ORC2 and
272 SIN3A were associated with LANA dots, but MeCP2 was not. The immunofluorescence assays in KSHV-
273 infected cells are in agreement with the CRISPR-PITA results, supporting the ability of CRISPR-PITA to
274 predict recruitment ability of proteins. While both ORC2 and SIN3A were recruited by LANA in CRISPR-
275 PITA, it seems that ORC2 was recruited to most LANA dots, while SIN3A was associated only with part
276 of LANA dots. This difference was also reflected in the Pearson's correlation coefficient, where the
277 correlation with SIN3A remained the same while the correlation with ORC2 increased upon directing
278 LANA to telomeres. Interestingly, this difference was also observed in infected cells, where SIN3A seems
279 to colocalize with only part of LANA-episome dots. The recruitment of GFP-LANA by scFv-MeCP2 also
280 suggests that CRISPR-PITA can be done without cell fixation or immunofluorescence, but directly via
281 detection of fluorescently-labeled proteins. This property might be more relevant in cases where CRISPR-
282 PITA is applied for screening purposes.

283 Targeting dCas9 to a repeat element, results in high protein concentration at specific nuclear locations. One
284 concern that might be raised is whether the recruitment we observed with CRISPR-PITA is specific or an
285 artifact of the high protein concentration. Our result that the same recruitment relations are detected also
286 when we directed dCas9 to a single locus (ERBB2 promoter), rules out this possibility. Regarding
287 specificity, we found that scFv-MeCP2 recruited the C-terminal of LANA, but not its N-terminal.
288 Interaction of LANA C-terminal domain with MeCP2 is in agreement with a previous study for LANA
289 (11). The related gamma-2 herpesvirus, herpesvirus saimiri (HVS) encodes for ORF73, a functional
290 homolog of KSHV encoded LANA (also known as ORF73). Interestingly, also HVS encoded ORF73
291 interacts with MeCP2 via its C-terminal domain (46). The lack of recruitment for the N-terminal domain of
292 LANA, indicated that recruitment is still specific and requires the interaction domain. Another support for
293 the specific recruitment by CRISPR-PITA is the lack of recruitment observed for GFP alone. A growing
294 list of nuclear proteins with intrinsically disordered regions and RNA/DNA binding properties can promote
295 liquid–liquid phase separation (LLPS); both LANA and MeCP2 possess this property (53, 54). Rett
296 syndrome MeCP2 mutants, including T158M are impaired in LLPS formation. Since T158M mutant still
297 can recruit LANA in CRISPR-PITA (although to a lesser extent), indicates that the recruitment we observed
298 is not dependent on LLPS formation.

299 The inability of LANA to recruit MeCP2, despite their documented interaction prompted us to test whether
300 MeCP2 can recruit LANA. Indeed, in CRISPR-PITA scFv-MeCP2 was able to recruit LANA. This result
301 comes in agreement with a previous study where MeCP2 recruited LANA to mouse heterochromatin foci
302 (12). This result also highlights the importance of a recruitment assay as recruitment is not always bi-

303 directional, and in many cases should be functionally unidirectional. One of LANA functions where
304 unidirectional recruitment seems essential, is LANA tethering of the viral episomal genome to the cell
305 chromosomes during cell division. Therefore, we tested the possible role of MeCP2 in KSHV episome
306 maintenance. We found that Rett syndrome mutant MeCP2, that cannot bind methylated DNA (T158M),
307 could not support KSHV latency. Our result suggests that in addition to LANA interaction with histones
308 (10), MeCP2 adds another layer to secure chromosome tethering (suggested model in **Fig. S4**). Similar to
309 KSHV encoded LANA, HVS encoded ORF73 has a critical role in viral episomal genome maintenance
310 (55). MeCP2 has been shown to be essential for tethering of the viral genomes by ORF73 to maintain HVS
311 latency (46). Therefore, our observation that MeCP2 is essential for episome maintenance, seems to be
312 conserved between KSHV and HVS. In this scenario LANA/ORF73 binds MeCP2 to anchor the viral
313 episomes to cellular chromosomes. If the anchor (MeCP2) is free (not bound to DNA/chromosome), this
314 may lead to viral loss. Therefore, in this case unidirectional recruitment is a matter of survival or extinction.

315 Do Rett syndrome patients are resistant to KSHV viral latency? *MeCP2* gene is located on the X-
316 chromosome, and Rett syndrome is found almost exclusively in females. Females, inherent two copies of
317 X-chromosome, one maternal and one paternal. During development one X-chromosome, is subjected to
318 X-chromosome inactivation, allowing expression of only one copy. Since females will present a mosaic
319 expression of the mutant and wt *MeCP2* alleles in different cells, it is reasonable to speculate that female
320 Rett syndrome patients will not be resistant to KSHV latent infection. It is important to note that in our
321 experiments, we used Single-cell derived clonal LCLs expressing either wt or mutant Rett syndrome
322 MeCP2 allele (45). Rett syndrome in males is very rare leading to in-utero lethality in most cases due to
323 having only a single copy of non-functional MeCP2. Another factor that contributes to the rarity of Rett
324 syndrome in males is their maternal origin of x-chromosome. While most MeCP2 mutations are sporadic,
325 and preferentially occur on the paternal x-chromosome (56, 57). So, only in these very rare cases of male
326 Rett syndrome, and only in those cases that the mutation disrupts DNA binding or the TRD domain of
327 MeCP2 we can expect a resistance to KSHV latency.

328 A nice example of directional recruitment is the case of MeCP2 that binds methylated DNA and recruits
329 co-repressor complexes including HDAC1 (20, 21). In this case we expect that MeCP2 should recruit
330 HDAC1, leading to transcription repression. On the other hand, HDAC1 is recruited by many transcription
331 factors to generate repressive chromatin. Therefore, we expect that it should not recruit MeCP2 to all the
332 chromosome locations it is recruited by other transcription repressors. Indeed, we found that scFv-MeCP2
333 was able to recruit HDAC1 to MeCP2-telomere-dots, but scFv-HDAC1 was unable to recruit MeCP2. How
334 come two proteins that interact with each other can generate unidirectional recruitment? MeCP2 is an

intrinsically disordered protein that is monomeric in solution even at high concentrations but dimerizes upon DNA binding (58, 59). Although CRISPR-PITA does not directly test the DNA binding of MeCP2, however the SunTag brings several MeCP2 molecules together therefore might force dimerization or binding to a DNA nearby, and by that can mimic DNA bound MeCP2. This might explain how the mutant MeCP2 T158M partially recruits LANA in CRISPR-PITA. Both LANA and HDAC1 interact with the MBD and TRD of MeCP2 (11, 21). In contrast, HP1α interacts with the N-terminal domain (amino acids 1–55) of MeCP2 (24). Therefore, while the TRD domain should be available for interaction only upon DNA binding and MeCP2 dimerization, we predicted that the N-terminal domain might be available for interaction also in its DNA-free form. Indeed, we found that HP1α is able to recruit MeCP2 to HP1α-telomere-dots. Another prediction of the model is that in the presence of a small DNA oligo for MeCP2 binding site, MeCP2 will bind the oligo, the interaction domain will become available and MeCP2 will be recruited by LANA. Indeed, in the presence of a small DNA oligo for MeCP2 binding site LANA was able to recruit MeCP2. Based on these characteristics and our CRISPR-PITA results we propose the following model; when MeCP2 is not associated with DNA it is a monomer and therefore the TRD and MBD are not available to interact with HDAC1 and LANA and therefore cannot be recruited by them. When MeCP2 binds methylated DNA its conformation changes so the TRD and MBD can bind and recruit HDAC1 and LANA. In this way, unidirectional recruitment of HDAC1 and LANA only to DNA bound MeCP2 is executed, while interaction with free MeCP2 is prevented (**Fig. 5C & D**). On the contrary, HP1α interacts with a different region, the N-terminus of MeCP2 that is available for binding also in its DNA-free state, and therefore HP1α can recruit MeCP2. It has been shown that phosphorylation at serine 229 (pS229) of MeCP2 strongly enhances the interaction between MeCP2 and HP1α (25). Our observation that HP1α can recruit MeCP2, may explain their observation that MeCP2 pS229 was enriched at the receptor tyrosine kinase gene *RET* promoter. In the future, it will be interesting to test the role of HP1α in the global distribution of MeCP2.

Materials and Methods

Cell culture. SLK cells (kindly provided by Don Ganem & Rolf Renne), NIH 3T3 cells (kindly provided by Oren Kobiler) and Vero-rKSHV.219 cells (kindly provided by Jeffrey Vieira) were cultured in Dulbecco's modified Eagle's medium (DMEM) supplemented with 10% fetal bovine serum (heat inactivated) and 100 U/ml penicillin, 100 µg/ml streptomycin, 2 mM L-glutamine, and 1 mM Sodium-Pyruvate in 5% CO_2 at 37°C. HCT and HCT Dnmt1-/- Dnmt3b -/- (DKO) cells (kindly provided by Bert Vogelstein) were grown in McCoy's 5A medium supplemented with the above-mentioned supplements.

BJAB and BCBL1 cells (kindly provided by Richard F. Ambinder), and LCLs (kindly provided by Uta Francke), were cultured in RPMI-1640 medium supplemented with 20% FBS and the above-mentioned supplements. Single-cell derived clonal LCLs expressing the wt or mutant Rett syndrome MeCP2 allele were established in the lab of Uta Francke (45).

Plasmids. pHRdSV40-dCas9-10xGCN4_v4-P2A-BFP (Addgene plasmid # 60903; http://n2t.net/addgene:60903; RRID:Addgene_60903) and pHR-scFv-GCN4-sfGFP-GB1-dWPRE (Addgene plasmid # 60907; http://n2t.net/addgene:60907; RRID:Addgene_60907) were a gift from Ron Vale (33). pgRNA-humanized was a gift from Stanley Qi (Addgene plasmid # 44248; http://n2t.net/addgene:44248; RRID:Addgene_44248) (27). The sgRNA targeting telomeres was cloned into pgRNA-humanized. The mCherry in the pgRNA-humanized was deleted by restriction digestion and ligation. LANA, HDAC1, HP1α and MeCP2 were PCR amplified and cloned into pHR-scFv-GCN4-sfGFP-GB1-dWPRE. scFv-LANA was further subcloned into pLIX_403, a gift from David Root (Addgene plasmid # 41395; http://n2t.net/addgene:41395; RRID:Addgene_41395). pEGFP-c2 from Clontech. GFP-LANA and LANA deletion plasmids were described previously (39, 60). For generation of MeCP2 (T158M) mutation RNA was isolated from LCL 487 (T158M) cell line by Qiagen RNeasy mini kit (cat no # 79656) and cDNA was prepared by maxima H minus first strand cDNA synthesis kit (cat no # K1682). A fragment of MeCP2 containing the T158M mutation was amplified by PCR and cloned in MeCP2-GFP plasmid (Addgene # 48078) and subsequently cloned into pHR-scFv-GCN4-sfGFP-GB1-dWPRE plasmid. MBD domain deleted MeCP2 was created by overlap extension PCR. Oligomerization mutant LANA was created by Q5 site directed mutagenesis kit (cat no# NEB E0554S). All primers can be found in supplementary primer list (**Table S1**). For ChIP assays we cloned the dCas9-5xSunTag from pCAG-dCas9-5xPlat2AflD, a gift from Izuho Hatada (Addgene plasmid # 82560 ; http://n2t.net/addgene:82560 ; RRID:Addgene_82560) (61), and sgRNA for ERBB2 promoter into lentiCRISPRv2 hygro, a gift from Brett Stringer (Addgene plasmid # 98291 ; http://n2t.net/addgene:98291 ; RRID:Addgene_98291) (62).

Immunofluorescence assay. $1X10^5$ cells were plated in 12 wells plate. Next day the cells were washed once with PBS and were transfected using PolyJet In Vitro DNA Transfection Reagent (SignaGene Laboratories Cat # SL100688) with the appropriate plasmids. In the day after $4X10^4$ cells were transferred into chamber slide cell culture glass 8 wells (SPL life Science LTD). Next day, the cells were washed once with PBS followed by fixation in 4% paraformaldehyde in PBS pH 7.4 for 10 minutes. After 3 washes with PBS, cells were permeabilized for 10 min with PBS containing 0.25% Triton X-100. Cells were washed 3 times with PBS and blocked with 1% BSA, 22.52 mg/mL glycine in PBST (PBS+ 0.1% Tween 20) for 45 min in 37° C. The slides were incubated for 1 hour with primary antibodies, followed by 3 washes with

PBS. Then, the slides were incubated with secondary antibodies for 1 hour and washed again 3 times with PBS and mounted with Vectaschield containing DAPI (Vector Laboratories, H-1500).

Antibodies. The following antibodies were used for immunofluorescence studies: Rat anti LANA (Advanced Biotechnologies, cat#13-210-100), Mouse anti LANA (Leica, NCL-HHV8-LNA), Mouse anti TRF2 (Merck, 05-521), Rabbit anti MeCP2 (Abcam, ab2828), Rabbit anti mSin3a/SIN3A (Abcam, ab3479), Mouse anti HA (Sigma H9658), Mouse anti ORC2 (MBL Life Science, M055-3), and Rabbit anti HDAC1 (Abcam, ab53091). Goat anti rabbit Alexa 488 (Abcam, ab150077), Goat anti Rat Alexa 488 (Abcam, ab150157), and Goat anti Mouse Alexa 594 (Abcam, ab150116). scFv-MeCP2, scFv-HP1α, and scFv-HDAC1 were detected with Mouse anti HA. scFv-LANA was detected by Mouse anti LANA, except in combination with TRF2 where Rat anti LANA was used. FLAG-LANA mutants (N+C, N, C) were detected with Rabbit anti FLAG (Sigma 7425).

Confocal imaging. Images were captured with Zeiss LSM780 inverted confocal microscope through a 63X objective with Z stack mode. Then, the middle stacks were selected and merged using Subset mode and Maximum Intensity Projection mode, respectively with Zenn software black edition. Processing and exporting of the resulted images was done with Zenn software blue edition.

Chromatin immunoprecipitation assay. ChIP assays were performed as described previously (63). Immunoprecipitation was performed with protein A/G Dynabeads (ThermoFisherScientific, #100-02D/100-04D) bound with Rat anti-LANA (Advanced Biotechnologies, cat#13-210-100), Rabbit anti-MeCP2 (Abcam, ab2828), or normal IgG (Millipore, PP64B) as a negative control. The immunoprecipitated chromatin was washed five times (with NaCl, lithium chloride and Tris-EDTA buffers), eluted and then purified using QIAquick kit (Qiagen, #28104) according to manufacturer's instructions.

LCL infection and maintenance assay. LCLs were infected with KSHV by co-culture (64). Briefly, Vero-rKSHV.219 cells (45) were induced with 1.25 mM sodium butyrate and 20 ng/ml 12-*O*-tetradecanoylphorbol-13-acetate (TPA) and after 48 h were cocultured with LCL cells (1:1 cell ratio) in RPMI 1640 medium for an additional 48 h. Medium containing the LCLs infected cells was collected and transferred to a new flask for an additional 48 h. Transferred again to a new flask, and at days 2, 7, 14, 24, cells were taken for FACS analysis to detect the number of GFP positive cells. At the same time points, genomic DNA was isolated with DNeasy blood and tissue kit (cat no # 69506) as per manufacturer instructions. Real time PCR was performed on genomic DNA using Fast SYBR green master mix (Applied

Biosystems), and results were analyzed with a CFX96 Touch real-time PCR detection system (Bio-Rad). GAPDH was used as an internal control.

Data availability

N.A. , as we did not generate large data sets.

Funding

This work was supported by grants from the Israel Science Foundation (https://www.isf.org.il) to M.S. (1365/21), and Research Career Development Award from the Israel Cancer Research Fund (https://www.icrfonline.org/) to M.S. (01282). We are grateful for the support of the Elias, Genevieve and Georgianna Atol Charitable Trust to the Daniella Lee Casper Laboratory in Viral Oncology. The funders had no role in study design, data collection and analysis, decision to publish, or preparation of the manuscript.

Acknowledgments

We would like to thank J Ron Vale, Stanley Qi, David Root, Izuho Hatada, Brett Stringer, and S. Diane Hayward for kindly providing plasmids, and Don Ganem, Rolf Renne, Jeffrey Vieira, Oren Kobiler, Richard F. Ambinder, Bert Vogelstein and Uta Francke for cell lines. We also would like to thank S. Diane Hayward for critically reading the manuscript, and Yosef Shaul for fruitful discussions.

References

1. Y. Chang *et al.*, Identification of herpesvirus-like DNA sequences in AIDS-associated Kaposi's sarcoma. *Science (New York, N.Y* **266**, 1865-1869 (1994).
2. C. Henke-Gendo, T. F. Schulz, Transmission and disease association of Kaposi's sarcoma-associated herpesvirus: recent developments. *Curr Opin Infect Dis* **17**, 53-57 (2004).
3. F. Ye, X. Lei, S. J. Gao, Mechanisms of Kaposi's Sarcoma-Associated Herpesvirus Latency and Reactivation. *Adv Virol* **2011** (2011).
4. L. Rainbow *et al.*, The 222- to 234-kilodalton latent nuclear protein (LNA) of Kaposi's sarcoma-associated herpesvirus (human herpesvirus 8) is encoded by orf73 and is a component of the latency-associated nuclear antigen. *J Virol* **71**, 5915-5921 (1997).
5. D. H. Kedes, M. Lagunoff, R. Renne, D. Ganem, Identification of the gene encoding the major latency-associated nuclear antigen of the Kaposi's sarcoma-associated herpesvirus. *J Clin Invest* **100**, 2606-2610 (1997).
6. A. Grundhoff, D. Ganem, The latency-associated nuclear antigen of Kaposi's sarcoma-associated herpesvirus permits replication of terminal repeat-containing plasmids. *J Virol* **77**, 2779-2783 (2003).

7. J. Hu, A. C. Garber, R. Renne, The latency-associated nuclear antigen of Kaposi's sarcoma-associated herpesvirus supports latent DNA replication in dividing cells. *J Virol* **76**, 11677-11687 (2002).
8. B. Kelley-Clarke, E. De Leon-Vazquez, K. Slain, A. J. Barbera, K. M. Kaye, Role of Kaposi's sarcoma-associated herpesvirus C-terminal LANA chromosome binding in episome persistence. *J Virol* **83**, 4326-4337 (2009).
9. E. De Leon Vazquez, K. M. Kaye, The internal Kaposi's sarcoma-associated herpesvirus LANA regions exert a critical role on episome persistence. *J Virol* **85**, 7622-7633 (2011).
10. A. J. Barbera *et al.*, The Nucleosomal Surface as a Docking Station for Kaposi's Sarcoma Herpesvirus LANA. *Science (New York, N.Y* **311**, 856-861 (2006).
11. S. Matsumura, L. M. Persson, L. Wong, A. C. Wilson, The latency-associated nuclear antigen interacts with MeCP2 and nucleosomes through separate domains. *J Virol* **84**, 2318-2330 (2010).
12. A. Krithivas, M. Fujimuro, M. Weidner, D. B. Young, S. D. Hayward, Protein interactions targeting the latency-associated nuclear antigen of Kaposi's sarcoma-associated herpesvirus to cell chromosomes. *J Virol* **76**, 11596-11604 (2002).
13. A. Viejo-Borbolla *et al.*, Brd2/RING3 interacts with a chromatin-binding domain in the Kaposi's Sarcoma-associated herpesvirus latency-associated nuclear antigen 1 (LANA-1) that is required for multiple functions of LANA-1. *J Virol* **79**, 13618-13629 (2005).
14. J. Hellert *et al.*, The 3D structure of Kaposi sarcoma herpesvirus LANA C-terminal domain bound to DNA. *Proceedings of the National Academy of Sciences of the United States of America* **112**, 6694-6699 (2015).
15. A. C. Garber, J. Hu, R. Renne, Latency-associated nuclear antigen (LANA) cooperatively binds to two sites within the terminal repeat, and both sites contribute to the ability of LANA to suppress transcription and to facilitate DNA replication. *J Biol Chem* **277**, 27401-27411 (2002).
16. J. F. Domsic, H. S. Chen, F. Lu, R. Marmorstein, P. M. Lieberman, Molecular basis for oligomeric-DNA binding and episome maintenance by KSHV LANA. *PLoS Pathog* **9**, e1003672 (2013).
17. A. De Leo *et al.*, LANA oligomeric architecture is essential for KSHV nuclear body formation and viral genome maintenance during latency. *PLoS Pathog* **15**, e1007489 (2019).
18. J. M. Hall, D. P. McDonnell, K. S. Korach, Allosteric regulation of estrogen receptor structure, function, and coactivator recruitment by different estrogen response elements. *Molecular endocrinology (Baltimore, Md* **16**, 469-486 (2002).
19. X. Nan, F. J. Campoy, A. Bird, MeCP2 is a transcriptional repressor with abundant binding sites in genomic chromatin. *Cell* **88**, 471-481 (1997).
20. P. L. Jones *et al.*, Methylated DNA and MeCP2 recruit histone deacetylase to repress transcription. *Nature genetics* **19**, 187-191 (1998).
21. X. Nan *et al.*, Transcriptional repression by the methyl-CpG-binding protein MeCP2 involves a histone deacetylase complex. *Nature* **393**, 386-389 (1998).
22. A. J. Bannister *et al.*, Selective recognition of methylated lysine 9 on histone H3 by the HP1 chromo domain. *Nature* **410**, 120-124 (2001).
23. M. Lachner, D. O'Carroll, S. Rea, K. Mechtler, T. Jenuwein, Methylation of histone H3 lysine 9 creates a binding site for HP1 proteins. *Nature* **410**, 116-120 (2001).

24. N. Agarwal *et al.*, MeCP2 interacts with HP1 and modulates its heterochromatin association during myogenic differentiation. *Nucleic acids research* **35**, 5402-5408 (2007).
25. M. L. Gonzales, S. Adams, K. W. Dunaway, J. M. LaSalle, Phosphorylation of distinct sites in MeCP2 modifies cofactor associations and the dynamics of transcriptional regulation. *Molecular and cellular biology* **32**, 2894-2903 (2012).
26. M. Jinek *et al.*, A programmable dual-RNA-guided DNA endonuclease in adaptive bacterial immunity. *Science (New York, N.Y* **337**, 816-821 (2012).
27. L. S. Qi *et al.*, Repurposing CRISPR as an RNA-guided platform for sequence-specific control of gene expression. *Cell* **152**, 1173-1183 (2013).
28. L. A. Gilbert *et al.*, CRISPR-mediated modular RNA-guided regulation of transcription in eukaryotes. *Cell* **154**, 442-451 (2013).
29. W. Deng, X. Shi, R. Tjian, T. Lionnet, R. H. Singer, CASFISH: CRISPR/Cas9-mediated in situ labeling of genomic loci in fixed cells. *Proceedings of the National Academy of Sciences of the United States of America* **112**, 11870-11875 (2015).
30. B. Chen *et al.*, Dynamic imaging of genomic loci in living human cells by an optimized CRISPR/Cas system. *Cell* **155**, 1479-1491 (2013).
31. T. Anton, S. Bultmann, H. Leonhardt, Y. Markaki, Visualization of specific DNA sequences in living mouse embryonic stem cells with a programmable fluorescent CRISPR/Cas system. *Nucleus* **5**, 163-172 (2014).
32. J. Duan *et al.*, Live imaging and tracking of genome regions in CRISPR/dCas9 knock-in mice. *Genome Biol* **19**, 192 (2018).
33. M. E. Tanenbaum, L. A. Gilbert, L. S. Qi, J. S. Weissman, R. D. Vale, A protein-tagging system for signal amplification in gene expression and fluorescence imaging. *Cell* **159**, 635-646 (2014).
34. M. E. Ballestas, P. A. Chatis, K. M. Kaye, Efficient persistence of extrachromosomal KSHV DNA mediated by latency-associated nuclear antigen. *Science (New York, N.Y* **284**, 641-644 (1999).
35. B. Kelley-Clarke *et al.*, Determination of Kaposi's sarcoma-associated herpesvirus C-terminal latency-associated nuclear antigen residues mediating chromosome association and DNA binding. *J Virol* **81**, 4348-4356 (2007).
36. J. Hellert *et al.*, A structural basis for BRD2/4-mediated host chromatin interaction and oligomer assembly of Kaposi sarcoma-associated herpesvirus and murine gammaherpesvirus LANA proteins. *PLoS Pathog* **9**, e1003640 (2013).
37. W. Stedman, Z. Deng, F. Lu, P. M. Lieberman, ORC, MCM, and Histone Hyperacetylation at the Kaposi's Sarcoma-Associated Herpesvirus Latent Replication Origin. *J. Virol.* **78**, 12566-12575 (2004).
38. S. C. Verma, K. Lan, T. Choudhuri, M. A. Cotter, E. S. Robertson, An autonomous replicating element within the KSHV genome. *Cell host & microbe* **2**, 106-118 (2007).
39. A. Krithivas, D. B. Young, G. Liao, D. Greene, S. D. Hayward, Human herpesvirus 8 LANA interacts with proteins of the mSin3 corepressor complex and negatively regulates Epstein-Barr virus gene expression in dually infected PEL cells. *J Virol* **74**, 9637-9645 (2000).
40. Q. Cai *et al.*, A unique SUMO-2-interacting motif within LANA is essential for KSHV latency. *PLoS Pathog* **9**, e1003750 (2013).

41. S. C. Verma, Q. Cai, E. Kreider, J. Lu, E. S. Robertson, Comprehensive analysis of LANA interacting proteins essential for viral genome tethering and persistence. *PloS one* **8**, e74662 (2013).
42. G. Stuber *et al.*, HHV-8 encoded LANA-1 alters the higher organization of the cell nucleus. *Molecular cancer* **6**, 28 (2007).
43. I. Rhee *et al.*, DNMT1 and DNMT3b cooperate to silence genes in human cancer cells. *Nature* **416**, 552-556 (2002).
44. R. P. Ghosh, R. A. Horowitz-Scherer, T. Nikitina, L. M. Gierasch, C. L. Woodcock, Rett syndrome-causing mutations in human MeCP2 result in diverse structural changes that impact folding and DNA interactions. *J Biol Chem* **283**, 20523-20534 (2008).
45. J. Traynor, P. Agarwal, L. Lazzeroni, U. Francke, Gene expression patterns vary in clonal cell cultures from Rett syndrome females with eight different MECP2 mutations. *BMC Med Genet* **3**, 12 (2002).
46. R. Griffiths, A. Whitehouse, Herpesvirus saimiri episomal persistence is maintained via interaction between open reading frame 73 and the cellular chromosome-associated protein MeCP2. *J Virol* **81**, 4021-4032 (2007).
47. P. C. Dedon, J. A. Soults, C. D. Allis, M. A. Gorovsky, A simplified formaldehyde fixation and immunoprecipitation technique for studying protein-DNA interactions. *Anal Biochem* **197**, 83-90 (1991).
48. V. Orlando, R. Paro, Mapping Polycomb-repressed domains in the bithorax complex using in vivo formaldehyde cross-linked chromatin. *Cell* **75**, 1187-1198 (1993).
49. A. S. Gonzalez-Serricchio, P. W. Sternberg, Visualization of C. elegans transgenic arrays by GFP. *BMC Genet* **7**, 36 (2006).
50. M. Higa *et al.*, TRF2 recruits ORC through TRFH domain dimerization. *Biochim Biophys Acta Mol Cell Res* **1864**, 191-201 (2017).
51. Y. Gao, M. Han, S. Shang, H. Wang, L. S. Qi, Interrogation of the dynamic properties of higher-order heterochromatin using CRISPR-dCas9. *Molecular cell* 10.1016/j.molcel.2021.07.034 (2021).
52. Y. Shin *et al.*, Liquid Nuclear Condensates Mechanically Sense and Restructure the Genome. *Cell* **175**, 1481-1491 e1413 (2018).
53. O. Vladimirova *et al.*, Phase separation and DAXX redistribution contribute to LANA nuclear body and KSHV genome dynamics during latency and reactivation. *PLoS Pathog* **17**, e1009231 (2021).
54. L. Wang *et al.*, Rett syndrome-causing mutations compromise MeCP2-mediated liquid-liquid phase separation of chromatin. *Cell Res* **30**, 393-407 (2020).
55. M. Calderwood, R. E. White, R. A. Griffiths, A. Whitehouse, Open reading frame 73 is required for herpesvirus saimiri A11-S4 episomal persistence. *J Gen Virol* **86**, 2703-2708 (2005).
56. M. Girard *et al.*, Parental origin of de novo MECP2 mutations in Rett syndrome. *Eur J Hum Genet* **9**, 231-236 (2001).
57. R. Trappe *et al.*, MECP2 mutations in sporadic cases of Rett syndrome are almost exclusively of paternal origin. *Am J Hum Genet* **68**, 1093-1101 (2001).
58. V. H. Adams, S. J. McBryant, P. A. Wade, C. L. Woodcock, J. C. Hansen, Intrinsic disorder and autonomous domain function in the multifunctional nuclear protein, MeCP2. *J Biol Chem* **282**, 15057-15064 (2007).

59. R. P. Ghosh, R. A. Horowitz-Scherer, T. Nikitina, L. S. Shlyakhtenko, C. L. Woodcock, MeCP2 binds cooperatively to its substrate and competes with histone H1 for chromatin binding sites. *Molecular and cellular biology* **30**, 4656-4670 (2010).
60. M. Fujimuro, S. D. Hayward, The latency-associated nuclear antigen of Kaposi's sarcoma-associated herpesvirus manipulates the activity of glycogen synthase kinase-3beta. *J Virol* **77**, 8019-8030 (2003).
61. S. Morita *et al.*, Targeted DNA demethylation in vivo using dCas9-peptide repeat and scFv-TET1 catalytic domain fusions. *Nature biotechnology* **34**, 1060-1065 (2016).
62. B. W. Stringer *et al.*, A reference collection of patient-derived cell line and xenograft models of proneural, classical and mesenchymal glioblastoma. *Sci Rep* **9**, 4902 (2019).
63. M. Shamay, M. Greenway, G. Liao, R. F. Ambinder, S. D. Hayward, De novo DNA methyltransferase DNMT3b interacts with NEDD8-modified proteins. *J Biol Chem* **285**, 36377-36386 (2010).
64. J. Myoung, D. Ganem, Infection of lymphoblastoid cell lines by Kaposi's sarcoma-associated herpesvirus: critical role of cell-associated virus. *J Virol* **85**, 9767-9777 (2011).
65. C. A. Schneider, W. S. Rasband, K. W. Eliceiri, NIH Image to ImageJ: 25 years of image analysis. *Nat Methods* **9**, 671-675 (2012).
66. A. Free *et al.*, DNA recognition by the methyl-CpG binding domain of MeCP2. *J Biol Chem* **276**, 3353-3360 (2001).

Figure legends

Figure 1. Schematic illustration of CRISPR-PITA. (A) Schematic illustration of dCas9-SunTag, sgRNA and scFv-LANA or other protein of interest (scFv-pY), and their binding to repetitive elements. **(B)** SLK cells were transfected with dCas9-SunTag, scFv-LANA, and sgTelomere as illustrated on the left of the images. Immunofluorescence assay was performed to detect LANA (red), and the nucleus was stained with DAPI (blue). Scale bar = 5 μm. **(C)** Schematic illustration of the CRISPR-PITA, targeting of scFv-LANA or any other protein of interest to the telomeres via dCas9. Then the recruitment of other nuclear proteins to these dots is evaluated via immunostaining.

Figure 2. LANA recruits ORC2 and SIN3A but not MeCP2. SLK cells were transfected with dCas9-SunTag, scFv-LANA, and sgTelomere expression plasmids as can be seen in the illustrations on the left. Immunofluorescence assays were performed to detect LANA (red) and ORC2 **(A)** mSin3a **(B)** or MeCP2 **(C)** (in green) cellular localization. The nucleus was stained with DAPI. Scale bar = 5 μm. The plots of the red, green and blue pixel intensities along the white arrow (in the left panels) are presented. (**D**) Pearson's correlation coefficient was determined by ImageJ (JACoP Pluing) (65) for 15 different cells in each treatment, and presented as box and whiskers (min to max). One-tailed *t* tests were performed (*, $P \leq 0.05$; **, $P \leq 0.01$; ***; $P \leq 0.001$).

Figure 3. MeCP2 recruits LANA. SLK cells were transfected with dCas9-SunTag, scFv-MeCP2, and sgTelomere in combination with GFP-LANA **(A)** or GFP **(B)** as illustrated on the left. Immunofluorescence assay was performed to detect scFv-MeCP2, or fluorescently labelled GFP-LANA and GFP. The nucleus was stained with DAPI. Scale bar = 5 μm. The plots of the red, green and blue pixel intensities along the white arrow (in the left panels) are presented. (**C**) SLK cells were transfected with FLAG-LANA N+C, FLAG-LANA C, or FLAG-LANA N, same as in A. Immunofluorescence assay was performed to detect both scFv-MeCP2 and LANA. (**D**) ChIP assay to detect LANA (left panel) and MeCP2 (right panel) association with the ERBB2 promoter following recruitment with sgRNA to this locus.

Figure 4. MeCP2 recruits HDAC1, while HDAC1 cannot recruit MeCP2. (A) HCT cells were transfected with dCas9-SunTag, scFv-MeCP2 and sgTelomere as illustrated on the left. Immunofluorescence assay was performed to detect HDAC1 (green) and scFv-MeCP2 (red). **(B-C)** HCT **(B)** and HCT DKO **(C)** cells were transfected same as in A but with scFv-HDAC1. Immunofluorescence assay was performed to detect MeCP2 (green) and scFv-HDAC1 (red). The nucleus was stained with DAPI. Scale bar = 5 μm. The plots of the red, green and blue pixel intensities along the white arrow (in the left panels) are presented.

665 **Figure 5. Availability of interacting domains determines recruitment directionality.** (**A**) schematic
666 presentation of MeCP2 and the interaction domains with LANA, HDAC1, and HP1α. Two Rett syndrome
667 mutants are indicated above. (**B**) SLK cells were transfected with dCas9-SunTag, scFv-HP1α, and
668 sgTelomere as illustrated on the left. Immunofluorescence assay was performed to detect MeCP2 (green)
669 and scFv-HP1α (red). The nucleus was stained with DAPI. Scale bar = 5 μm. Schematic illustrations of the
670 model for free (**C**) and DNA bound (**D**) MeCP2 are presented. (**E**) Schematic presentation of the experiment
671 in (**F**). (**F**) SLK cells were transfected with dCas9-SunTag, scFv-LANA, and sgTelomere. The next day
672 they were kept un-transfected or transfected with MeCP2 site binding oligo (66), or control Oligo.
673 Immunofluorescence assay was performed to detect MeCP2 (green) and scFv-LANA (red). The plots of
674 the red, green and blue pixel intensities along the white arrow (in the left panels) are presented.

675 **Figure 6. Rett syndrome mutant MeCP2 T158M cannot support KSHV latency. (A-B)** LCLs were
676 infected with rKSHV.219 and GFP-positive cells by FACS analysis (**A**) or amount of KSHV DNA by
677 qPCR (**B**) were evaluated at the indicated time points. Experiments were performed with biological
678 triplicates. (**C**) Immunofluorescence assay was performed to detect GFP-LANA (green) and scFv- MeCP2
679 (red). The nucleus was stained with DAPI. Scale bar = 5 μm. (**D**) NIH 3T3 cells were transfected with
680 GFP-LANA and wt MeCP2, T158M mutant, or del-MBD. Immunofluorescence assay was performed same
681 as in C. The plots of the red, green and blue pixel intensities along the white arrow (in the left panels) are
682 presented.

683

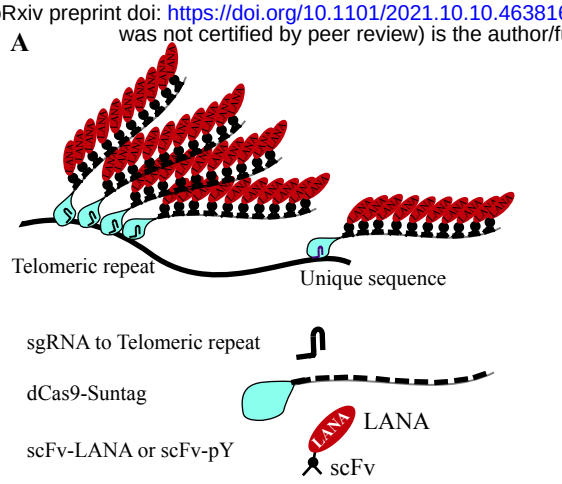

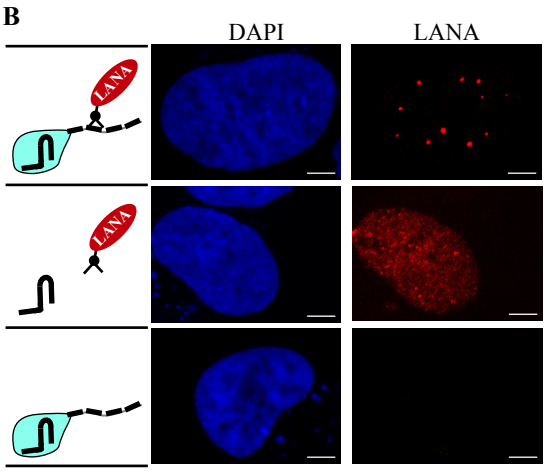

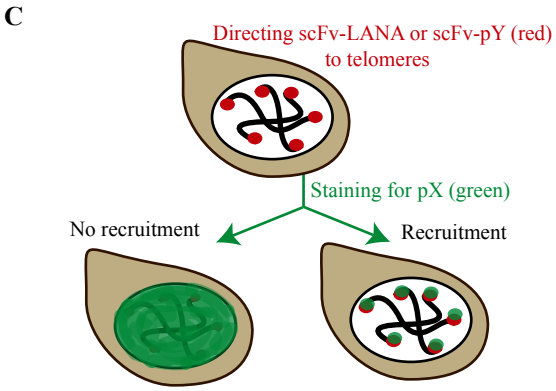

Fig.1

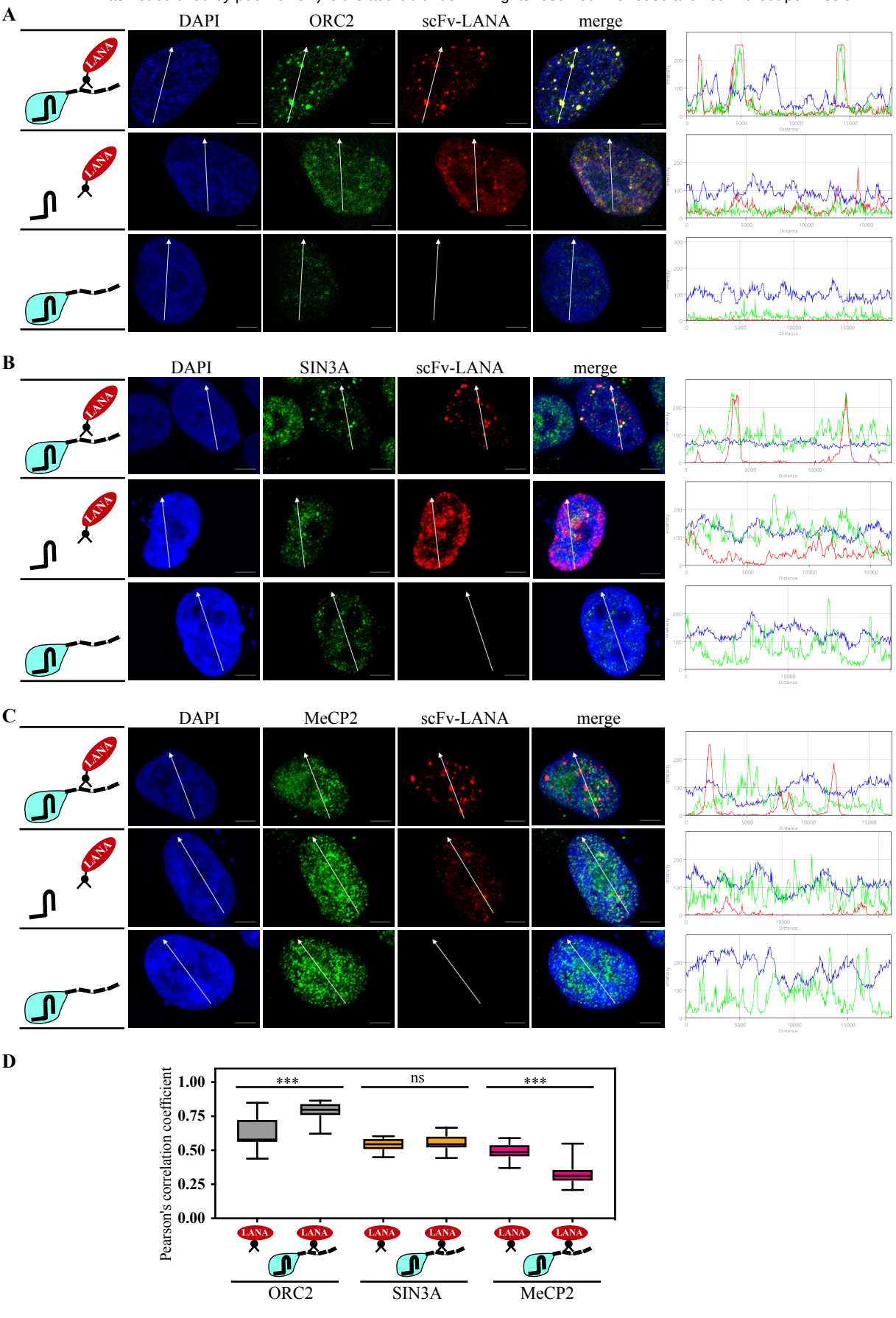

Fig.2

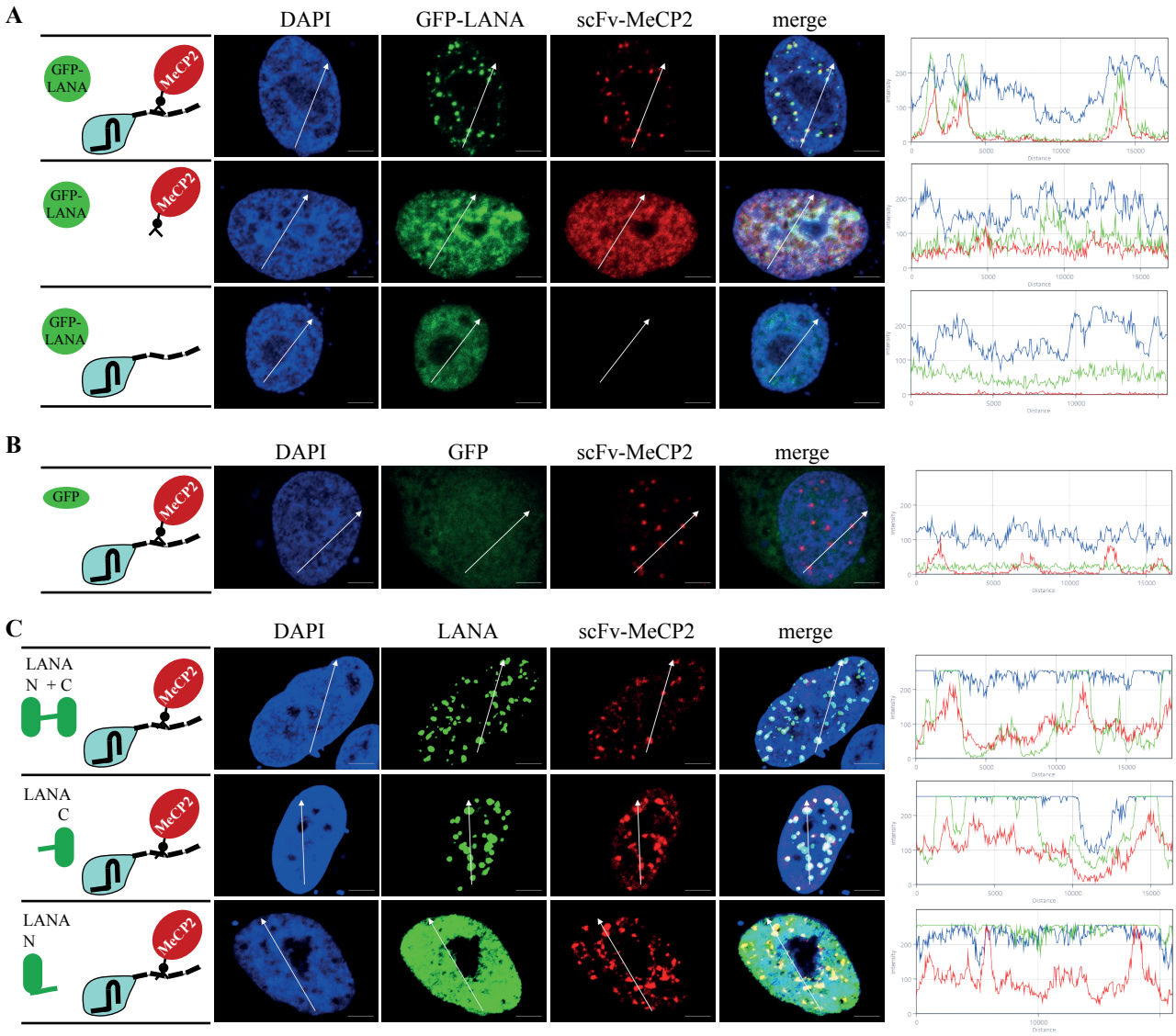

Fig.3

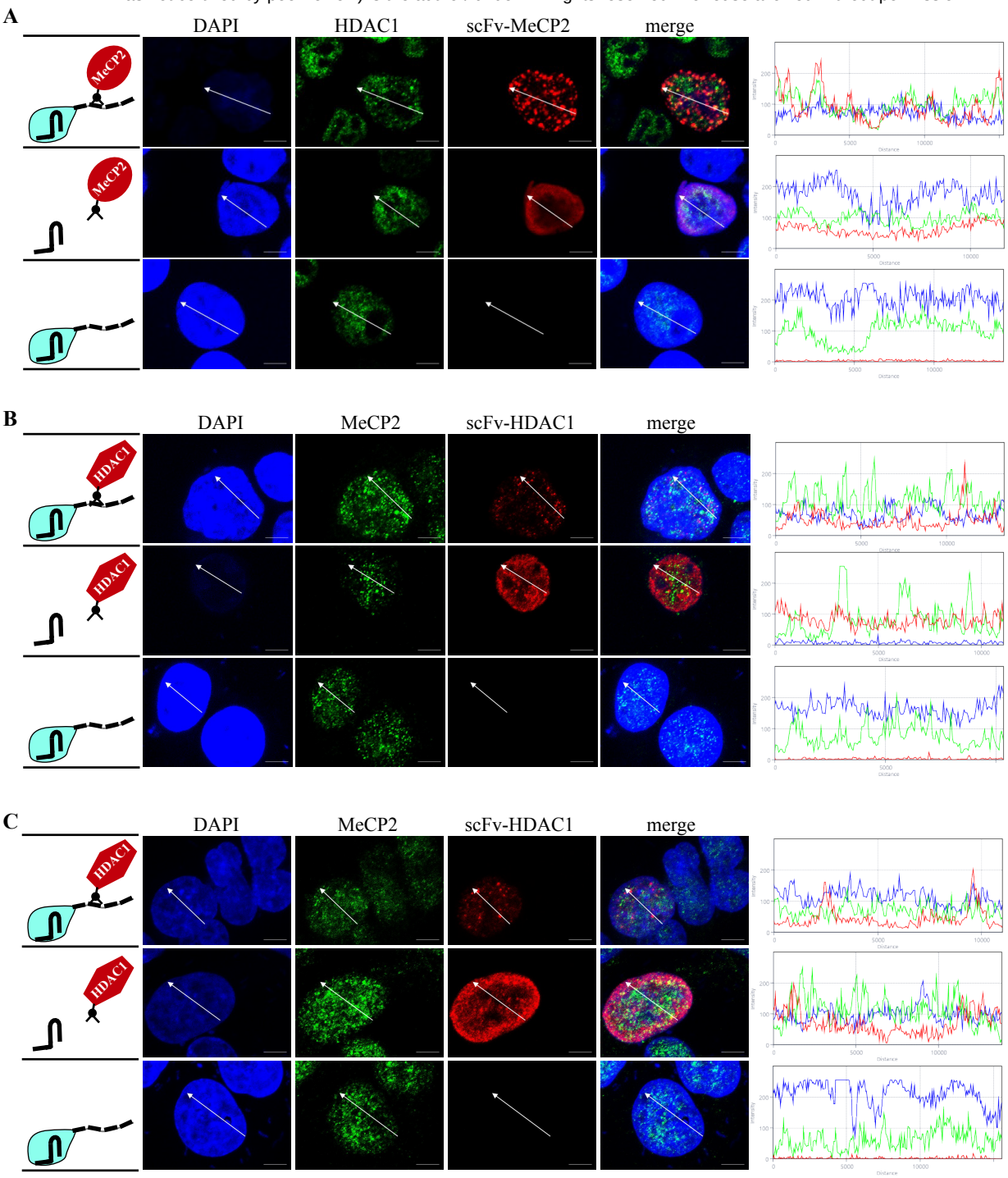

Fig.4

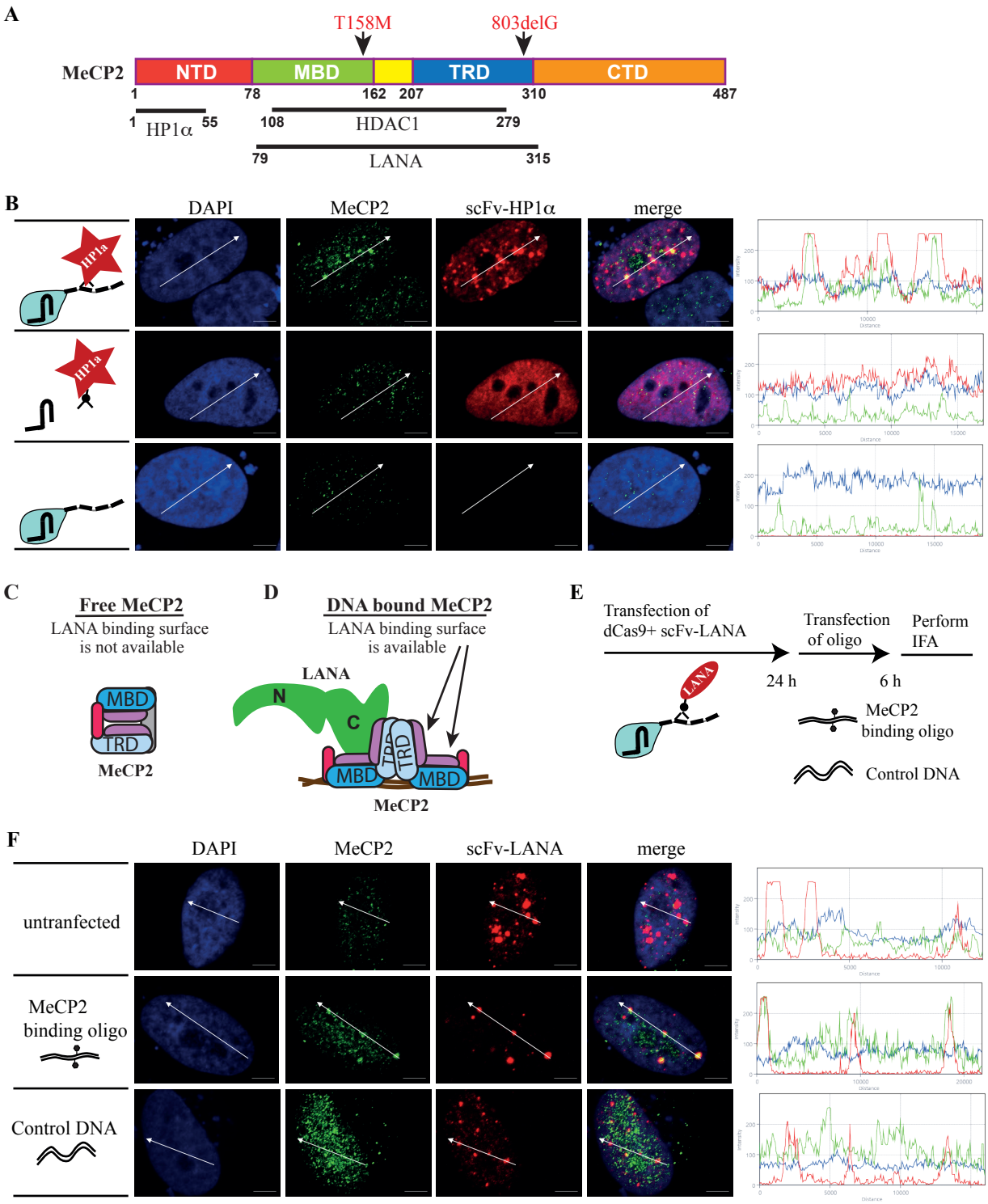

Fig.5

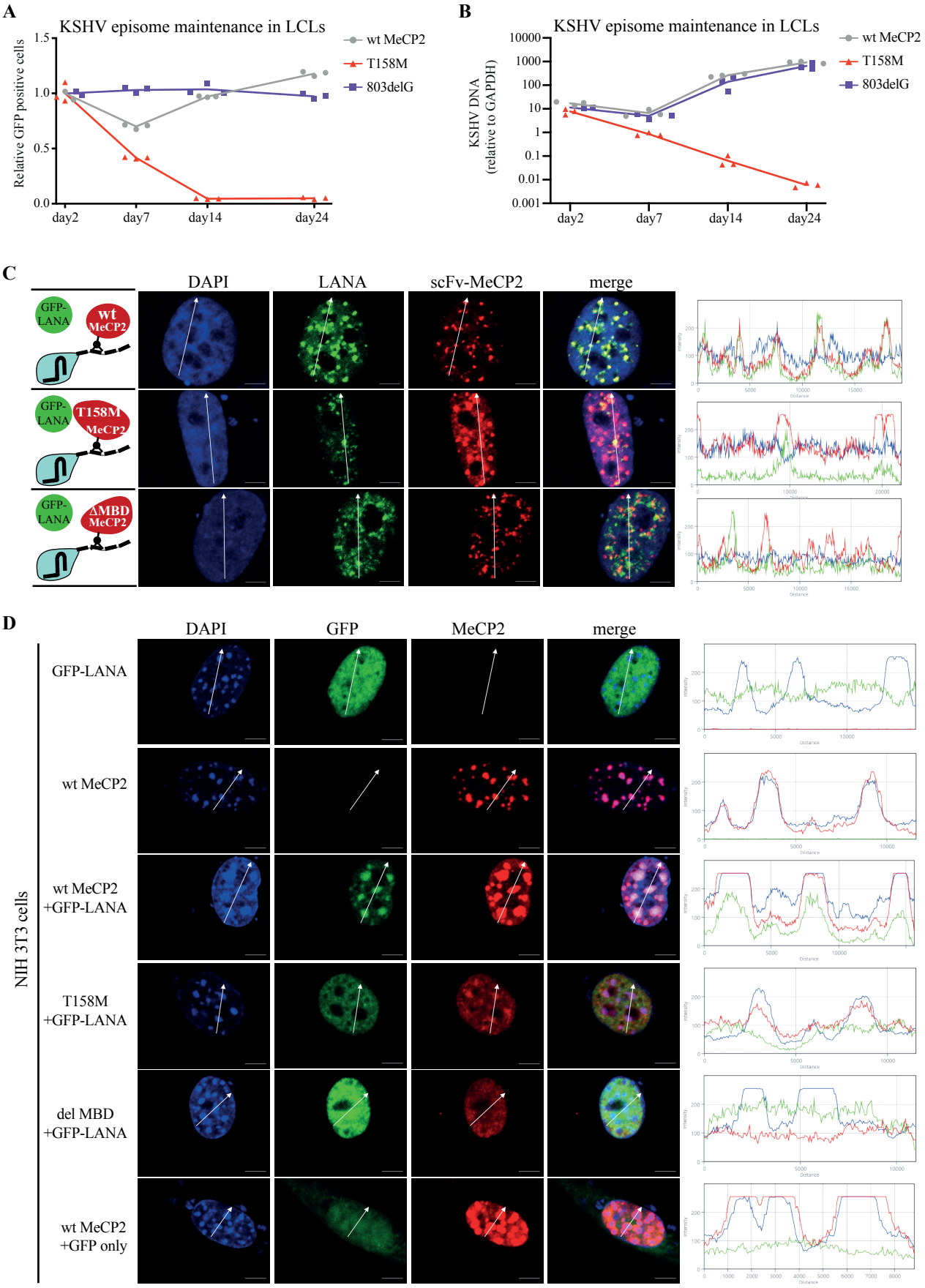

Fig.6